Original Article

MOLECULAR METABOLISM

Rasal2 deficiency reduces adipogenesis and occurrence of obesity-related disorders

Xiaoqiang Zhu [1,3], Simin Xie [1], Tian Xu [1,2], Xiaohui Wu [1,*], Min Han [1,3]

ABSTRACT

Objective: Identification of additional regulatory factors involved in the onset of obesity is important to understand the mechanisms underlying this prevailing disease and its associated metabolic disorders and to develop therapeutic strategies. Through isolation and analysis of a mutant, we aimed to uncover the function of a Ras-GAP gene, Rasal2 (Ras protein activator like 2), in the development of obesity and related metabolic disorders and to obtain valuable insights regarding the mechanism underlying the function.

Methods: An obesity-based genetic screen was performed to identify an insertional mutation that disrupts the expression of Rasal2 (*Rasal2*$^{PB/PB}$ mice). Important metabolic parameters, such as fat mass and glucose tolerance, were measured in *Rasal2*$^{PB/PB}$ mice. The impact of Rasal2 on adipogenesis was evaluated in the mutant mice and in 3T3-L1 preadipocytes treated with Rasal2 siRNA. Ras and ERK activities were then evaluated in Rasal2-deficient preadipocytes or mice, and their functional relationships with Rasal2 on adipogenesis were investigated by employing Ras and MEK inhibitors.

Results: *Rasal2*$^{PB/PB}$ mice showed drastic decrease in Rasal2 expression and a lean phenotype. The mutant mice displayed decreased adiposity and resistance to high-fat diet induced metabolic disorders. Further analysis indicated that Rasal2 deficiency leads to impaired adipogenesis *in vivo* and *in vitro*. Moreover, while Rasal2 deficiency resulted in increased activity of both Ras and ERK in preadipocytes, reducing Ras, but not ERK, suppressed the impaired adipogenesis.

Conclusions: Rasal2 promotes adipogenesis, which may critically contribute to its role in the development of obesity and related metabolic disorders and may do so by repressing Ras activity in an ERK-independent manner.

Keywords Ras; ERK; Ras-GAP; Glucose tolerance; High-fat diet; Diabetes

1. INTRODUCTION

Obesity, which has grown to be a world-wide epidemic, has multiple metabolic consequences such as type II diabetes, hepatic steatosis, dyslipidemia, cardiovascular diseases, and certain types of cancer [1]. Identification of pathways that modulate the development of obesity will provide critical information regarding new therapeutic approaches to obesity and its associated diseases.

Ras proteins are known to play fundamental roles in cell growth and proliferation [2]. Potential important roles of Ras in regulating obesity-related cellular processes have been suggested by several studies, with certain caveats to be examined. First, transgenic mice over-expressing (8-fold) H-Ras specifically in adipose tissue displayed a remarkable decrease in fat mass [3], which suggested a potential role of Ras in repressing adipogenesis. However, since the study was performed under non-physiological conditions, the result is subjected to alternative explanations. Second, human and mouse genetic studies revealed that loss-of-function mutations in the Kinase suppressor of Ras 2 (*KSR2*) gene are associated with obesity in human and cause obesity in mice [4]. However, since KSR2 has been shown to bind to and regulate the activity of AMPK, in addition to its known role in promoting the Ras-Raf-MEK-ERK signaling pathway [5–7], further studies are required to determine if KSR2 acts through the Ras pathway to repress obesity. Finally, genetic ablation of docking protein 1 (Dok1), a protein known to repress Ras function by recruiting Ras-GAP to Ras [8,9], inhibits adipogenesis and causes mice to be lean [10]. This result also suggests a role of Ras in repressing adipogenesis. Therefore, additional studies are desirable to validate this role and fully understand this potentially important regulatory mechanism, which may lead to identification of potential new therapeutic targets.

Rasal2 was identified as a Ras-GAP through cancer-related studies [11–13]. A genome-wide association study has linked SNP rs10913469 (*Sec16B-Rasal2*) to increased body mass index in humans [14]. Two independent studies reproduced this association in Chinese and certain Mexican populations [15,16]. These data suggest potential roles of Sec16B or Rasal2 in the development of obesity. Genetic studies using mouse genetics should be effective and

[1]State Key Laboratory of Genetic Engineering and National Center for International Research of Development and Disease, Institute of Developmental Biology and Molecular Medicine, Collaborative Innovation Center for Genetics and Development, School of Life Sciences, Fudan University, Shanghai 200433, China [2]Howard Hughes Medical Institute, Department of Genetics, Yale University School of Medicine, New Haven, CT 06536, USA [3]Howard Hughes Medical Institute, Department of Molecular, Cellular, and Developmental Biology, University of Colorado, Boulder, CO 80309, USA

*Corresponding author. E-mail: xiaohui_wu@fudan.edu.cn (X. Wu).

Received February 22, 2017 • Accepted March 15, 2017 • Available online 18 March 2017

http://dx.doi.org/10.1016/j.molmet.2017.03.003

important to determine the role of Rasal2 in obesity-related cellular processes, which may elucidate the role of Ras in obesity.

In a screen for obesity-associated mutants based on systematic *Piggybac* (PB) transposon insertional mutagenesis, we identified a mutant strain with drastically reduced expression of *Rasal2*. This mutant strain provides an excellent mouse model to explore the roles of endogenous Ras proteins. The mutant mice display a lean phenotype with improvements in glucose tolerance, insulin sensitivity, and other metabolic parameters related to obesity. We carried out in-depth analysis to reveal the roles and mechanisms of Rasal2 in the development of obesity.

2. MATERIALS AND METHODS

2.1. Animals

FVB Mice were housed under 12/12 h light/dark cycles with free access to water and normal chow diet or 60 kcal% high-fat diet (Research Diets, Inc). All animal-related experiments were performed in accordance with guidelines from the Institute of Developmental Biology and Molecular Medicine Institutional Animal Care and Use Committee.

2.2. Indirect calorimetry

Mice were individually housed under room temperature (21 °C) with free access to food and water. Locomotor activity, O_2 consumption, and CO_2 production were measured using a Promethion Metabolic Measurement System.

2.3. Histology

For frozen section, tissues were dissected and fixed in 10% formalin solution overnight. The samples were then dehydrated in 30% sucrose and embedded in OCT. 10 μm sections were collected. For Oil-Red-O staining, cells or slides were fixed for 1 h at room temperature with 10% formalin before stained with Oil-Red-O as described previously [17]. After taking photos, the Oil-Red-O was extracted with isopropanol for spectrophotometric measurement at 510 nm.

2.4. Glucose tolerance test (GTT) and insulin tolerance test (ITT)

For GTT, 12-week old mice were fasted for 16—18 h, and injected with D-glucose (2 g/kg, intraperitoneally). Tail vein blood was sampled and analyzed with an Onetouch Ultra blood glucose monitoring system (LifeScan) at 0, 30, 60, 90, and 120 min after injection, respectively. For ITT, 12-week old mice were fasted for 6 h before being injected with insulin (Humulin, Lilly) (0.75 U/kg, intraperitoneally). 0, 15, 30, 45, 60 min after injection, tail vein blood was sampled for glucose determination.

2.5. siRNA transfection of 3T3-L1 preadipocytes and adipogenesis induction

Cells were maintained in expansion medium [High glucose DMEM (Gibco, 11965118) supplemented with 10% FCS (Gibco, 16170078), 1% Penicillin-Streptomycin (Gibco, 10378016)]. Transfection of siRNA against *Rasal2* was performed as previously described [18]. In brief, 3T3-L1 preadipocytes were trypsinized, resuspended in expansion medium, then seeded into 24-well plates and transfected with siRNA by Lipofectamine RNAiMAX (Life Technologies). Two days after reaching confluency, cells were induced with a defined adipogenic cocktail [High glucose DMEM (Sigma, 11965118) supplemented with 10% FBS (Gibco, 16000044), 1% Penicillin-Streptomycin (Gibco, 10378016), 5 μg/ml insulin (Sigma, I0259), Dexamethasone (Sigma, D1756), and 0.5 mM 3-Isobutyl-1-methylxanthine (IBMX) (Sigma, I7018)] for 2 days, then raised in the maintenance medium [High glucose DMEM (11965118) supplemented with 10% FBS (Gibco, 16000044), 1% Penicillin-Streptomycin (Gibco, 10378016), and 5 μg/ml insulin (Sigma, I0259)] for additional 4 days. The sequences of Rasal2 siRNA could be found in Table S2.

2.6. Assay of Ras activity

Cells were lysed on ice in the lysis buffer containing 25 mM HEPES (pH 7.5), 150 mM NaCl, 1% NP-40, 0.25% sodium deoxycholate, 10% glycerol, 25 mM NaF, 10 mM $MgCl_2$, 1 mM EDTA, 1 mM sodium orthovanadate, protease inhibitor (Roche). 500 mg of cell lysate was incubated at 4 °C with 5 μg glutathione-Sepharose beads (Upstate biotechnology) coupled with a glutathione S-transferase fusion protein corresponding to Ras binding domain of human Raf-1. The bead-bound proteins were analyzed by Western blotting.

2.7. Farnesyl Thiosalicylic Acid (FTS) and U0126 treatment of 3T3-L1 preadipocytes

FTS was dissolved in ethanol (5 mM). Cells were treated with adipogenic cocktail added with 10 μM or 50 μM FTS for 2 days, then incubated with the maintenance medium containing 10 μM or 50 μM FTS for 2 days. After that, cells were cultured in maintenance medium for an additional 2 days.

U0126 was reconstituted in DMSO (10 mM). For U0126 treatment, cells were stimulated with adipogenic cocktail for 12 h, then switched to adipogenic cocktail supplemented with 10 nM, 50 nM, 250 nM, or 1250 nM U0126 for 36 h. The choice of applying the inhibitor at 12 h post-induction was based on a previous study that showed ERK acts to promote C/EBPα and PPARγ expression (which, in turn, enhances adipogenesis), and PPARγ expression was induced at 12 h post-induction [27]. Subsequently, cells were maintained in maintenance medium containing the same concentration of U0126 for 2 more days. The cells were then cultured in maintenance medium for an additional 2 days.

2.8. Real-time PCR

Tissues or cells were homogenized in Trizol (Invitrogen), and then total RNA was extracted following the standard protocol. One μg RNA was used for complementary DNA synthesis using a Reverse Transcription kit (Takara, RR047A). Real-time PCR was performed by using Brilliant II FAST SYBR QPCR Master Mix (Agilent) in LyghtCycler™ 480 system (Roche). 36B4 or 18s RNA was used as the internal control. Primers used in real-time PCR can be found in Table S2. Some primer sequences are from PrimerBank [19].

2.9. Western blotting

Protein was extracted from cells or tissues by using RIPA buffer [50 mM Tris-HCl (pH 8.0), 150 mM NaCl, 1% NP-40, 0.5% sodium deoxycholate and 0.1% SDS] supplemented with protease inhibitor (Roche) and phosphatase inhibitor (Roche). Protein was separated by SDS-PAGE and transferred to PVDF membranes. Antibodies used were: Phospho-ERK (Thr202/Tyr204) (Cell Signaling), ERK (Cell Signaling), Rasal2 (ProteinTech), beta-actin (Santa Cruz), beta-tubulin (Sigma), and GAPDH (Sigma).

2.10. Statistics

All data were analyzed with a two-tailed unpaired/paired Student's t-test and expressed as mean ± s.e.m. Statistical significance is represented by asterisks: *$p < 0.05$, **$p < 0.01$, ***$p < 0.001$. All n values refer to biological repeats.

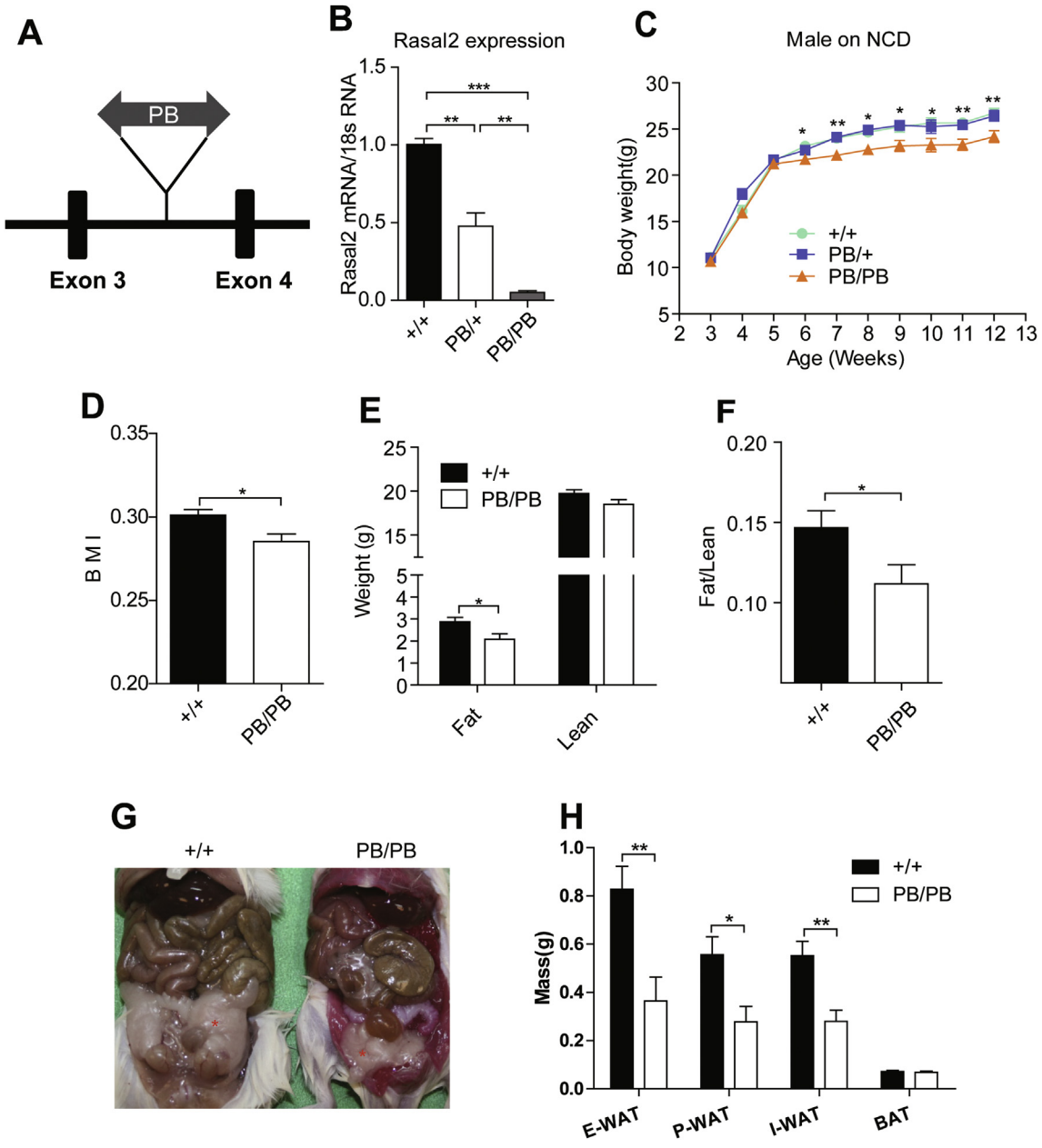

Figure 1: *Rasal2* expression was disrupted by the PB insertion and *Rasal2*$^{PB/PB}$ mice show decreased adiposity. (A) A *PB* element insert in between exon3 and exon4 of the *Rasal2* gene. (B) *Rasal2* mRNA level was drastically reduced by the *PB* insertion in whole embryos (n = 3 for each group). (C) Body weight of wild-type controls, *Rasal2*$^{PB/+}$, and *Rasal2*$^{PB/PB}$ mice fed normal chow diet (NCD) (n = 6–9 for each group). (D) *Rasal2*$^{PB/PB}$ mice have lower body mass index (BMI) than wild-type controls (n = 5 for each group). (E) The fat and lean mass of *Rasal2*$^{PB/PB}$ and wild-type control mice fed NCD (+/+, n = 9; *PB/PB*, n = 7) measured by nuclear magnetic resonance (NMR). (F) Fat to lean mass ratio of *Rasal2*$^{PB/PB}$ and wild-type control mice fed NCD (+/+, n = 9; *PB/PB*, n = 7). (G) Representative photographs of epididymal adipose of *Rasal2*$^{PB/PB}$ and wild-type control mice. Red stars indicate the epididymal adipose. (H) Mass of various adipose depots from *Rasal2*$^{PB/PB}$ and wild-type control mice fed NCD (n = 6 for each group). E-WAT: epididymal adipose tissue, P-WAT: peri-renal adipose tissue, I-WAT: inguinal adipose tissue, BAT: brown adipose tissue. 12-week-old mice were used unless otherwise stated. See also Figure S1. *p < 0.05, **p < 0.01, ***p < 0.001. Data were analyzed with a two-tailed unpaired Student's t-test and expressed as mean ± s.e.m.

3. RESULTS

3.1. PB element insertion disrupted the expression of *Rasal2* gene and rendered mice to be lean

A previous study found *Rasal2* mRNA is present in brain, lung, heart, liver, kidney, testis, and skeletal muscle [11]. Using quantitative-RT-PCR, we detected *Rasal2* mRNA in six additional tissues including white adipose tissue (WAT) and brown adipose tissue (BAT) (Figure S1A), indicating a ubiquitous expression of Rasal2 in mouse. A *Rasal2* mutant mouse strain (*Rasal2*$^{PB/PB}$ mice) was identified by a systematic *piggyBac* (PB) transposon insertional mutagenesis [20,21]. In this mutant strain, inverse PCR [20] revealed a single copy of PB element inserts in the third intron of *Rasal2* (Figure 1A). *Rasal2* mRNA level in homozygous (*Rasal2*$^{PB/PB}$) embryo was reduced to less than 10% of that of wild-type controls (Figure 1B).

On a normal chow diet (NCD), male *Rasal2*$^{PB/PB}$ mice showed modestly but significantly decreased body weight at 6 weeks of age and remained lower for the duration of analysis (Figure 1C). Female

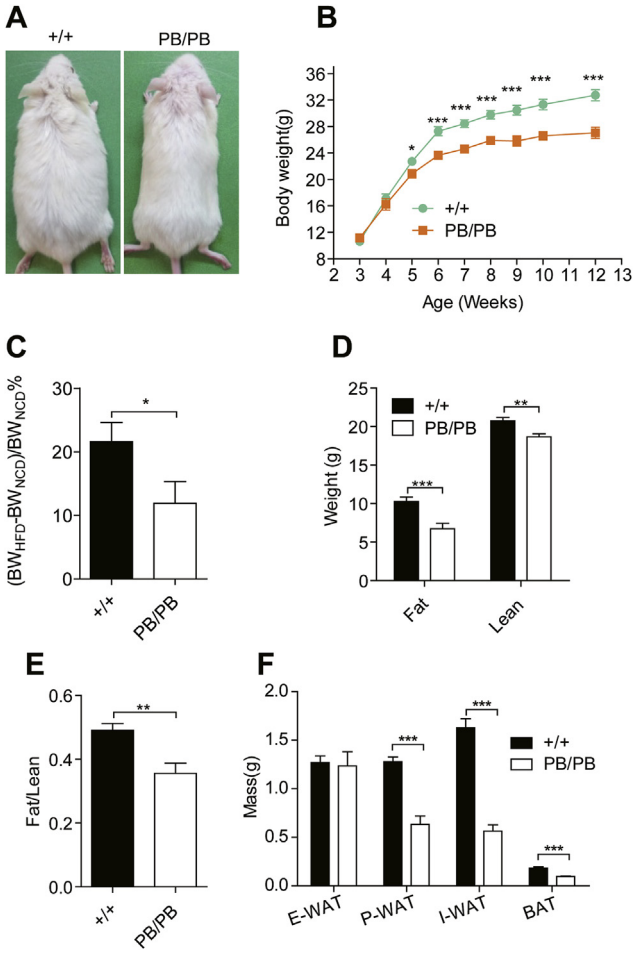

Figure 2: *Rasal2*$^{PB/PB}$ mice are partially resistant to HFD-induced obesity. (A) Representative photographs of *Rasal2*$^{PB/PB}$ and wild-type control mice on high-fat diet (HFD). (B) Body weight of *Rasal2*$^{PB/PB}$ and wild-type control mice on HFD ($n \geq 5$ for each group). (C) HFD-induced body weight gain of *Rasal2*$^{PB/PB}$ and wild-type control mice ($n = 5$ for each group). (D) The fat and lean mass of *Rasal2*$^{PB/PB}$ and wild-type control mice fed HFD ($n = 14$ for each group) measured by NMR. (E) Fat mass to lean mass ration of *Rasal2*$^{PB/PB}$ and wild-type control mice fed HFD ($n = 14$ for each group). (F) Mass of various adipose depots from *Rasal2*$^{PB/PB}$ and wild-type control mice fed HFD ($n = 5$ for each group). E-WAT: epididymal adipose tissue, P-WAT: peri-renal adipose tissue, I-WAT: inguinal adipose tissue, BAT: brown adipose tissue. 12-week-old mice were used unless otherwise stated. See also Figure S1. *$p < 0.05$, **$p < 0.01$, ***$p < 0.001$. Data were analyzed with a two-tailed unpaired Student's t-test and expressed as mean ± s.e.m.

Rasal2$^{PB/PB}$ mice also manifested a decrease in body weight since the age of 8 weeks (Figure S1B). The body mass index (BMI) of male *Rasal2*$^{PB/PB}$ mice was significantly lower than that of wild-type control mice (Figure 1D). Nuclear magnetic resonance (NMR) analysis revealed that *Rasal2*$^{PB/PB}$ mice had significantly less fat mass, with only a subtle change in lean mass (Figure 1E and Figure S1C), resulting in a lower fat mass to lean mass ratio (Figure 1F). To further confirm this result from NMR analysis, we dissected and assessed the mass of several adipose depots. We observed that the mass of epididymal-WAT, peri-renal WAT, and inguinal WAT were significantly lower in *Rasal2*$^{PB/PB}$ mice, while the mass of brown adipose tissue remained unchanged (Figure 1G and H). Taken together, these data show that *Rasal2*$^{PB/PB}$ mice are leaner.

To address if food intake or physical activity played a role in the lean phenotype that we observed, we tested several parameters. We did not observe significant differences in food intake (Figure S1D), locomotor activity (Figure S1F), energy expenditure (Figure S1H), or respiratory exchange rate (RER) (Figure S1J) between *Rasal2*$^{PB/PB}$ mice and wild-type controls fed NCD.

3.2. *Rasal2*$^{PB/PB}$ mice are partially resistant to high-fat diet-induced obesity

To investigate the potential resistance of *Rasal2*$^{PB/PB}$ mice to high-fat diet (HFD) induced obesity, male *Rasal2*$^{PB/PB}$ mice and wild-type control mice were challenged with HFD started at weaning. HFD-fed male *Rasal2*$^{PB/PB}$ mice had significantly lower body weight from the age of 5 weeks (Figure 2A and B). Importantly, the HFD-induced body weight gain relative to NCD feeding is significantly lower in *Rasal2*$^{PB/PB}$ mice (Figure 2C), indicating *Rasal2*$^{PB/PB}$ mice are partially resistant to HFD. The NMR analysis revealed that both the fat and lean mass of *Rasal2*$^{PB/PB}$ mice are lower than those of wild-type control mice (Figure 2D). As the change in fat mass is more severe than in lean mass, the fat-mass to lean-mass ratio is still lower in *Rasal2*$^{PB/PB}$ mice (Figure 2E). We dissected and weighed various adipose pads and found that wild-type control mice have significantly less peri-renal WAT, inguinal WAT, and brown adipose tissue than *Rasal2*$^{PB/PB}$ mice (Figure 2F). It is interesting to note that, while the differences in the mass of inguinal white and brown adipose between wild-type and *Rasal2*$^{PB/PB}$ mice were further augmented by HFD feeding, the difference in the mass of epididymal white adipose disappeared when mice were fed HFD (Figure 2F), implying different adipose depots of *Rasal2*$^{PB/PB}$ mice have different responses to HFD feeding.

On HFD, *Rasal2*$^{PB/PB}$ mice displayed comparable food intake, locomotor activity, and RER to wild-type control mice (Figure S1E, G, and K). However, we observed significantly higher energy expenditure in *Rasal2*$^{PB/PB}$ mice (Figure S1I). The increase in energy expenditure is more likely a consequence rather than a cause of the leanness, as the mutant mice were already leaner than wild-type mice when fed NCD, a condition under which the mutant mice and wild-type controls show similar energy expenditure (Figure S1H).

3.3. *Rasal2* deficiency protects mice from HFD-induced metabolic disorders

Obesity is a key risk factor for type II diabetes [1]. Therefore, we investigated the glucose homeostasis of *Rasal2*$^{PB/PB}$ mice. While only marginal differences were seen when mice were fed NCD (Figure S2A–D), male *Rasal2*$^{PB/PB}$ mice fed HFD exhibited significantly enhanced glucose tolerance (Figure 3A and B) and insulin sensitivity (Figure 3C and D). Consistently, we observed lower fasting serum insulin level when mice were fed HFD, but no significant difference was observed when mice were fed NCD (Figure 3E and Figure S2E). We also observed significantly lower serum triglycerides and cholesterol levels (Figure 3F and G). Hepatic steatosis is known to be associated with obesity [22]. Histological analysis revealed that *Rasal2*$^{PB/PB}$ mice were protected from HFD-induced hepatic steatosis (Figure 3H), accompanied by lower liver weight (Figure 3I). The circulating alanine transaminase (ALT) level, a commonly used indicator of liver damage, was notably lower in *Rasal2*$^{PB/PB}$ mice when fed HFD (Figure 3J). Importantly, the circulating ALT level of *Rasal2*$^{PB/PB}$ mice fed HFD was comparable to that of mice fed NCD (Figure 3J), indicating that *Rasal2*$^{PB/PB}$ mice were almost completely protected from HFD-induced liver damage under these conditions. Albumin, calcium, urea nitrogen, and total protein levels in the blood of *Rasal2*$^{PB/PB}$ mice were also altered when compared with wild-type control mice (Table S1).

Obesity has also been linked to chronic and low-grade inflammation in white adipose, which constitutes a significant contributor to insulin

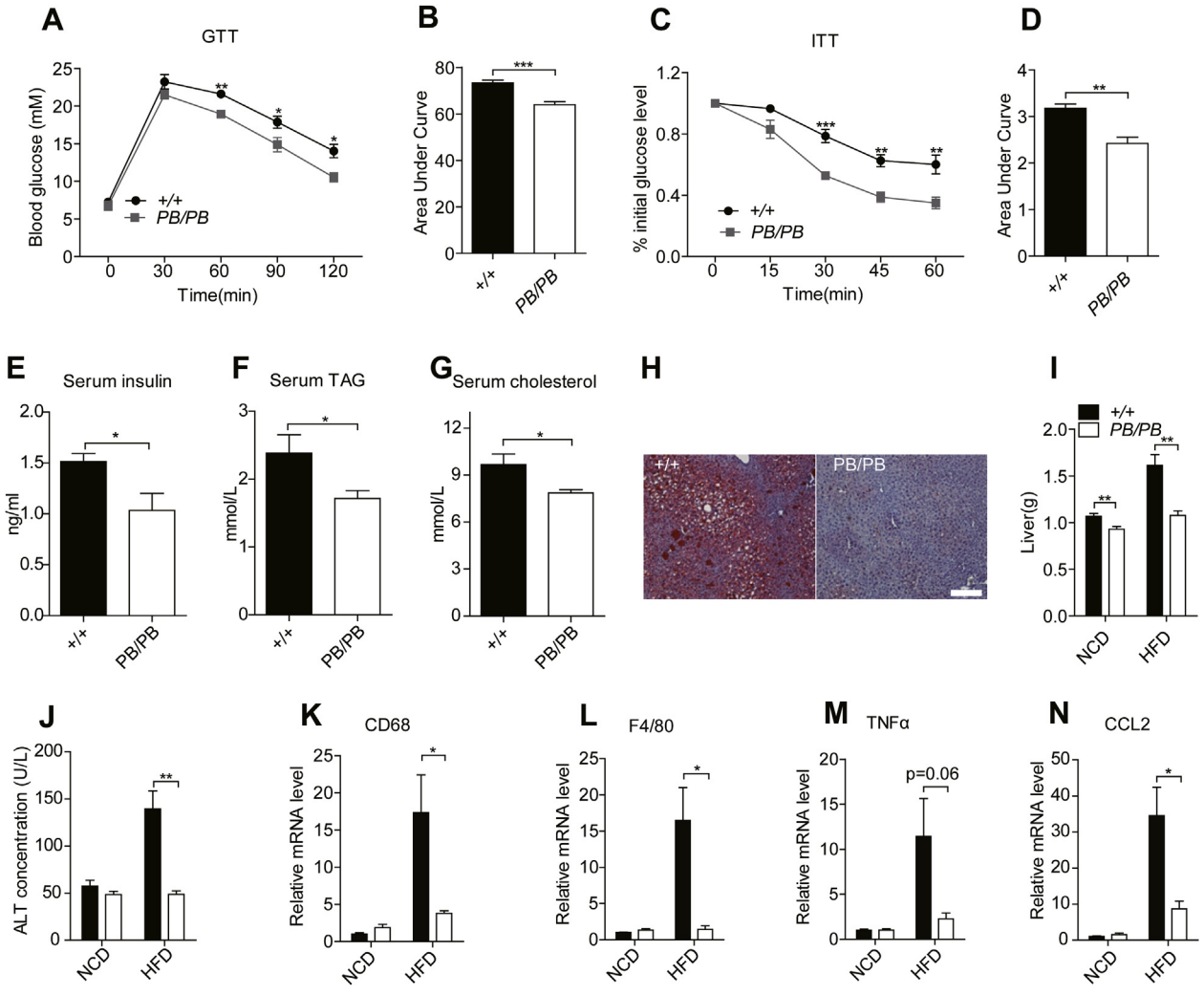

Figure 3: *Rasal2*$^{PB/PB}$ mice are protected against HFD-induced metabolic disorders. (A and B) Glucose tolerance test (GTT) of *Rasal2*$^{PB/PB}$ and wild-type control mice fed HFD (n = 5–6 for each group). (C and D) Insulin tolerance test (ITT) of *Rasal2*$^{PB/PB}$ and wild-type control mice fed HFD (n = 5 for each group). (E–G) Serum insulin levels (E) triglycerides (TAG) levels (F) and cholesterol levels (G) of *Rasal2*$^{PB/PB}$ and wild-type control mice fed HFD (n = 5 for each group). (H) Liver triglycerides content of mice fed HFD determined by Oil-Red-O staining. Scale bar, 500 μm. (I) Liver weight of *Rasal2*$^{PB/PB}$ and wild-type control mice (n = 5–6 for each group). (J) Concentration of circulating alanine transaminase (ALT) in *Rasal2*$^{PB/PB}$ mice and wild-type control mice (n = 4–5 for each group). (K–N) Expression of indicated macrophage markers and pro-inflammatory cytokines in the white adipose of *Rasal2*$^{PB/PB}$ mice and wild-type control mice (n = 3–5 for each group). 12-week-old mice were used unless otherwise stated. See also Figure S2. *p < 0.05, **p < 0.01, ***p < 0.001. Data were analyzed with a two-tailed unpaired Student's t-test and expressed as mean ± s.e.m.

resistance and subsequent type II diabetes [23]. To evaluate the inflammation state in the white adipose tissue of *Rasal2*$^{PB/PB}$ mice, we analyzed the expression of macrophage markers CD68 and F4/80 and the pro-inflammatory genes TNFα and CCL2 by quantitative PCR. On NCD, the white adipose inflammatory state, as reflected by the expression of these genes, was comparable between *Rasal2*$^{PB/PB}$ mice and wild-type control mice (Figure 3K–N). HFD feeding induced a robust increase in the expression of CD68 and F4/80 as well as TNFα and CCL2 in wild-type mice (Figure 3K–N). Strikingly, the induction of all of these genes was prominently suppressed in *Rasal2*$^{PB/PB}$ mice (Figure 3K–N). Obesity is also known to be associated with M2 macrophage infiltration into white adipose, even though the M1 to M2 macrophages ratio is typically decreased under this condition [24]. As expected, *Rasal2* deficiency abrogated HFD-induced M2 macrophage infiltration in white adipose tissue (Figure S2F–H). Further analysis showed that the inflammation state was comparable between *Rasal2*$^{PB/PB}$ mice and wild-type control mice prior to the divergence of body weight (Figure S2I–K), suggesting that the lower inflammation in white adipose of *Rasal2*$^{PB/PB}$ mice fed HFD might be a consequence of decreased adiposity.

Taken together, these results suggest that *Rasal2* deficiency not only results in the lean phenotype but also suppresses HFD-induced metabolic disorders.

3.4. Rasal2 deficiency impairs adipogenesis *in vivo* and *in vitro*

Consistent with the substantially decreased expression of Rasal2 in *Rasal2*$^{PB/PB}$ embryos, the mRNA and protein levels of Rasal2 are drastically reduced in white adipose tissue (Figure 4A and B). Given the decreased fat mass in *Rasal2*$^{PB/PB}$ mice, we examined adipose development at early stage of life (P2). At this stage, we observed that the subcutaneous fat of *Rasal2*$^{PB/PB}$ mice is much thinner than that in the wild-type control mice, indicating compromised *in vivo* adipogenesis (Figure 4C). Thus, we examined the potential cell-autonomous roles of Rasal2 in adipogenesis by knocking down the expression of Rasal2 with

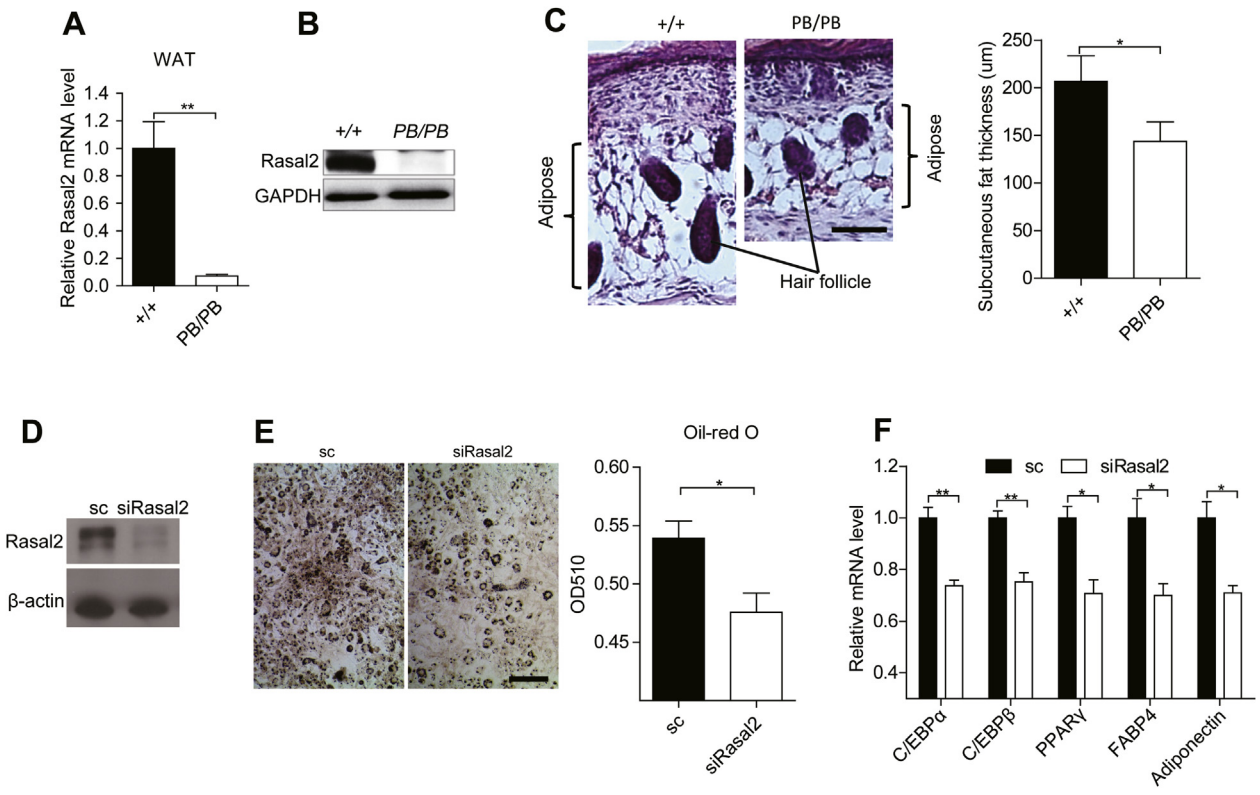

Figure 4: Rasal2 deficiency impairs adipogenesis *in vivo* and *in vitro*. (A and B) mRNA level (A) and protein level (B) of Rasal2 in the white adipose tissue of *Rasal2*$^{PB/PB}$ mice and wild-type control mice (n = 3 for each group). (C) Subcutaneous adipose of P2 *Rasal2*$^{PB/PB}$ mice and wild-type control mice (n = 3 for each group). (D) Western blot showing siRNA against Rasal2 efficiently reduced the expression of Rasal2 protein in 3T3-L1 preadipocytes. (E–F) Knockdown of Rasal2 compromised the adipogenesis of 3T3-L1 preadipocytes indicated by Oil-Red-O staining (n = 4 for each group) (E) and the expression of indicated adipocyte marker genes (n = 3 for each group) (F). *$p < 0.05$, **$p < 0.01$, ***$p < 0.001$. Data were analyzed with a two-tailed unpaired Student's t-test except that data in (C) were analyzed with a two-tailed paired Student's t-test. See also Figure S2. All data were expressed as mean ± s.e.m.

siRNA in 3T3-L1 preadipocytes (Figure 4D). The result shows that Rasal2 knockdown caused a significant reduction of adipogenesis, reflected by decreased Oil-Red-O staining (Figure 4E) and lower expression of adipocyte marker genes (Figure 4F). These *in vivo* and *in vitro* data indicate that, Rasal2 deficiency impairs adipogenesis, which is likely a critical contributor to the lean phenotype of *Rasal2*$^{PB/PB}$ mice.

The metabolic phenotypes of *Rasal2*$^{PB/PB}$ mice could also be caused by defects in other tissues. We examined the expression of genes involved in energy expenditure in several tissues including liver, skeletal muscle, brown adipose, epididymal white adipose, as well as inguinal white adipose of HFD fed *Rasal2*$^{PB/PB}$ and wild-type control mice and found significant increases in the expression of thermogenic genes only in inguinal adipose tissue (Figure S2L–P). When mice were fed NCD, these thermogenic genes in inguinal white adipose were expressed at comparable levels between genotypes (Figure S2Q). Therefore, the increase of thermogenic gene expression is likely a consequence but not a cause of the lean phenotype. Nevertheless, this increase may still contribute to the resistance to HFD induced disorders in *Rasal2*$^{PB/PB}$ mice. In addition, the phosphorylation levels of JAK2 and STAT3 in hypothalamus were also measured, and no significant differences were noted between genotypes (Figure S2R).

3.5. Rasal2 deficiency represses adipogenesis by augmenting Ras activity

Rasal2 is a known Ras-GAP in several cancer cell lines [12], while the potential Ras-GAP activity of Rasal2 in adipocytes or preadipocytes has not been determined. To address this question, we analyzed 3T3-L1 preadipocytes and observed a significant increase in Ras-GTP level when Rasal2 was knocked down by siRNA (Figure 5A). In agreement with this finding, the phosphorylation of ERK, a main Ras effector protein, is also modestly but significantly increased (Figure 5B). In white adipose tissue, though we did not detect an obvious alteration in ERK phosphorylation on basal state (Figure S3A), ERK phosphorylation was higher than in wild-type control mice after 15-minute insulin stimulation (Figure S3A). These data indicate that Rasal2 has a repressive role on Ras in preadipocytes and adipose. If increased Ras activity is responsible for the impaired adipogenesis of Rasal2-knockdown preadipocytes, then reducing Ras activity may suppress the phenotype. We found that the impaired adipogenesis in Rasal2-knockdown 3T3-L1 preadipocytes was fully reversed when a Ras inhibitor, Farnesyl Thiosalicylic Acid (FTS, 50 μM), was used to block Ras activity (Figure 5C, D, and E). The Ras inhibitor Manumycin A was also capable of partially rescuing the defective adipogenesis (Figure S3B). Therefore, Rasal2 likely promotes adipogenesis in preadipocytes by repressing Ras activity.

In the white adipose tissue of *Rasal2*$^{PB/PB}$ mice and Rasal2-knockdown 3T3-L1 preadipocytes, we noted an increase in ERK phosphorylation level (Figure S3A and Figure 5B). Given that over-activation of ERK blocks late stage of adipogenesis by repressing PPARγ activity [25,26], this increase would be consistent with the idea that the repressive effect of Rasal2 deficiency on adipogenesis in these cells is executed through raising ERK activity. In 3T3-L1 preadipocytes, PPARγ

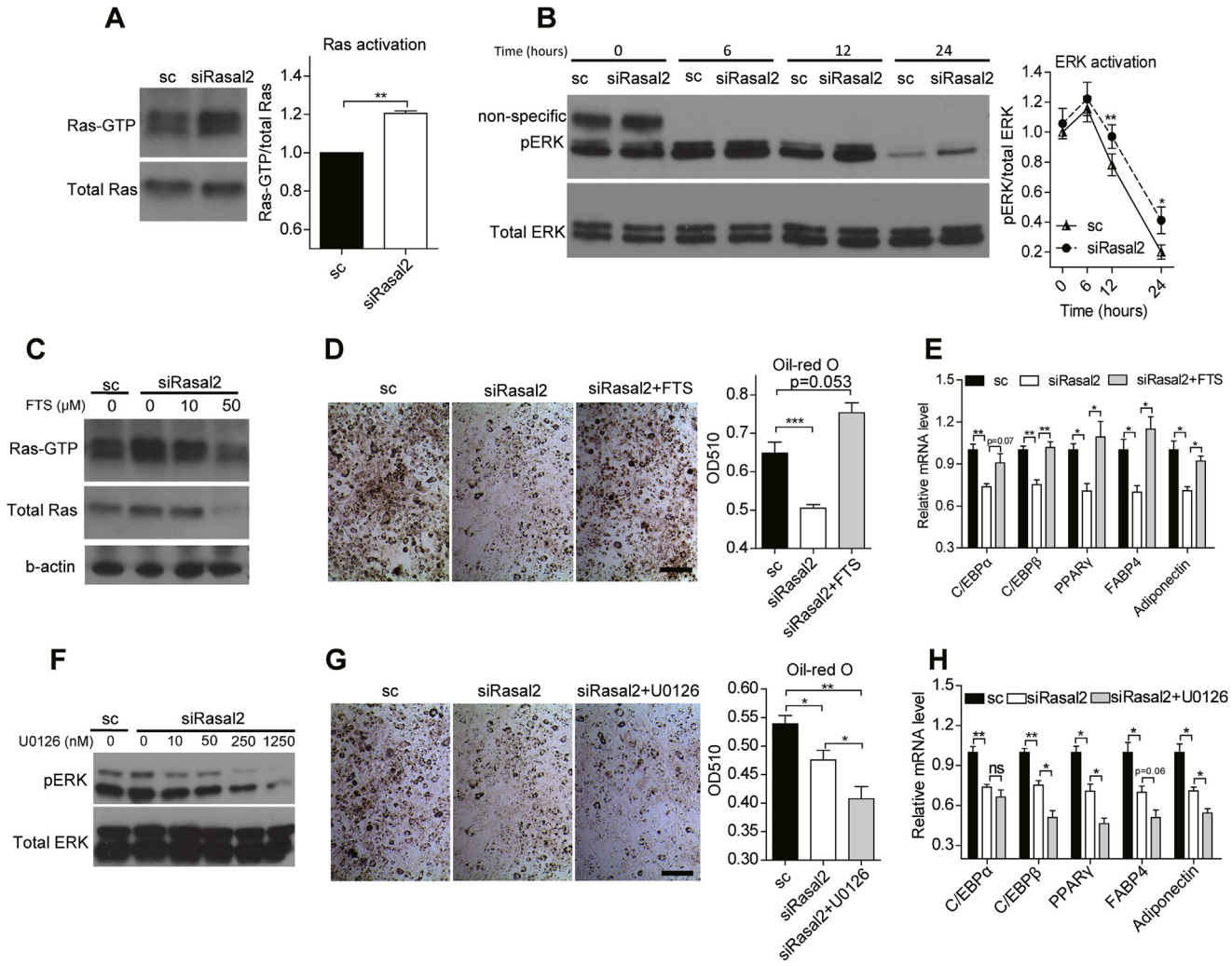

Figure 5: Rasal2 modulates adipogenesis through Ras proteins. (A) Higher Ras-GTP level in Rasal2-knockdown 3T3-L1 preadipocytes. 3T3-L1 preadipocytes were stimulated with adipogenic cocktail for 15 min before performing the Ras activation assay (n = 3 for each group). (B) The phosphorylated ERK level is increased in Rasal2-knockdown 3T3-L1 preadipocytes. 3T3-L1 preadipocytes were treated with adipogenic cocktail for indicated time. (n = 4 for each group). (C) Western blot showing that the Ras inhibitor Farnesyl Thiosalicylic Acid (FTS) blocks Ras activity in a concentration-dependent manner. (D and E) 50 μM FTS reverses the impaired adipogenesis of Rasal2-knockdown preadipocytes indicated by Oil-Red-O staining (n = 4 for each group) (D) and the expression of indicated adipocyte marker genes (n = 3 for each group) (E). (F) Western blot showing that the MEK inhibitor U0126 blocked ERK phosphorylation in a concentration-dependent manner. U0126 was added to culture at 12 h post adipogenic-induction, phosphorylated ERK level was evaluated 6 h later. (G and H) 10 μM U0126 failed to rescue the defective adipogenesis of Rasal2-knockdown 3T3-L1 preadipocytes indicated by Oil-Red-O staining (n = 4 for each group) (G) and the expression of indicated adipocyte marker genes (n = 3 for each group) (H). See also Figure S3. *p < 0.05, **p < 0.01, ***p < 0.001. Data were analyzed with a two-tailed unpaired Student's t-test and expressed as mean ± s.e.m.

expression was induced from 12 h post-induction [27]; therefore, we asked whether blocking ERK activity after PPARγ was induced could suppress the deficiency in adipogenesis. Using the MEK inhibitor U0126 (10 nM) to block ERK activity (U0126 was added 12 h post-induction), the increase in phosphorylated ERK was effectively suppressed in Rasal2-knockdown 3T3-L1 preadipocytes. (Figure 5F and Figure S3C). In contrast to the hypothesized repressive role of ERK, the U0126 treatment failed to rescue the impaired adipogenesis (Figure 5G and H). Instead, it further down-regulated adipogenesis (Figure 5G and H). We also tried to block ERK activity in Rasal2-knockdown 3T3-L1 preadipocytes with U0126 (10 nM) at the beginning of adipogenic induction and did not observe significant rescue of the impaired adipogenesis (Figure S3D). This result suggests that Rasal2 might regulate adipogenesis in an ERK-independent manner. However, we should point out that the MEK-ERK pathway acts on multiple aspects of cellular events related to cell differentiation and lipid homeostasis. In addition, there could be caveats associated with using U0126 to inhibit ERK activity, despite that it is widely used. Therefore, the suggestion from our data that Rasal2 promotes adipogenesis by an ERK-independent mechanism may not be viewed as a firm conclusion.

4. DISCUSSION

In this study, we demonstrate that *Rasal2* deficiency leads to lower adiposity and an increase in resistance to HFD-induced obesity. In addition, *Rasal2* deficiency ameliorates numerous obesity-related metabolic disorders, including glucose intolerance, insulin resistance, and hepatic steatosis. We found no detectable changes in food

intake or locomotor activity in these *Rasal2*$^{PB/PB}$ mice, either on HFD or NCD. We also showed that the lean phenotype of *Rasal2*$^{PB/PB}$ mice is unlikely a consequence of altered energy expenditure. We provide evidence that deficiency of Rasal2 impairs the development of adipocytes *in vivo* and *in vitro*, which may be a critical cause of the lean phenotype of *Rasal2*$^{PB/PB}$ mice.

As expected, the deficiency of Rasal2 results in higher activation of Ras and ERK. While we showed that the elevation of Ras activity is responsible for the limited adipogenesis, our observation does not support that this regulation is mediated by ERK. ERK has been shown to play significant and seemingly complex roles in adipogenesis [27–30]. It was demonstrated that ERK activation plays a positive role in the early stage of adipogenesis by promoting the expression of C/EBPα and PPARγ [27]. Other studies provided evidence that in late stage of adipogenesis, ERK represses adipogenesis by phosphorylating PPARγ, which leads to inhibition of PPARγ transcriptional activity [10,25,26], which may be consistent with data showing that ERK activity is down-regulated after PPARγ was induced [27]. However, another study provided evidence that ERK activity is required not only for the initiation of adipogenesis but also for the maturation of adipocyte [31], which blurred the picture regarding what the precise role of ERK in late stage adipogenesis is. In our study, we showed that, after PPARγ was induced, reduction of ERK activity in Rasal2-deficient preadipocytes by a MEK inhibitor U0126 further reduced adipogenesis, instead of suppressing the defect. This result suggests that the observed deficiency in adipogenesis in Rasal2-deficient preadipocytes is not due to the observed modest increase of ERK activity, implicating that this increased ERK activity has not reached the level that could inhibit adipogenesis by repressing PPARγ transcriptional activity. Instead, the observed further down-regulation of adipogenesis indicates a positive role of the observed modest increase of ERK activity in adipogenesis at this stage, which is in agreement with the finding that ERK is essential for adipocyte maturation [31]. The indication from this analysis suggests that the Rasal2 function in regulating adipogenesis may be mediated by an ERK-independent mechanism. Therefore, the downstream effector of Ras that mediates its inhibition on adipogenesis in Rasal2-deficient preadipocytes is yet to be determined.

Despite of our finding that Rasal2 deficiency compromises adipogenesis, we did not exclude the possibility that Rasal2 may also function non-autonomously in other tissues, such as the hypothalamus and muscle, to impact the development of obesity, as we only performed limited analyses to explore the functions of Rasal2 in these tissues. Nevertheless, the analyses of the Rasal2 mutant mice, in which the Rasal2 expression is dramatically reduced, but not eliminated, may implicate Rasal2 as a potential therapeutic target to combat obesity-related disorders.

FUNDING

This work was supported in part by grants from Chinese Hi-tech Research and Development Project (863) [2012AA022401], Natural Science Foundation of China (NSFC) [81570756, 81170789], Shanghai Municipal Science and Technology Commission (STCSM) [15XD1500500], and Howard Hughes Medical Institute.

AUTHOR CONTRIBUTION

Xiaoqiang Zhu designed and performed experiments, analyzed data, and wrote the manuscript. Simin Xie maintained the mice and provided reagents. Tian Xu provided materials and analyzed data. Xiaohui Wu and Min Han provided materials, analyzed data, edited the manuscript, and co-supervised the study.

ACKNOWLEDGEMENTS

We thank Drs. Yin Leng, Li Jin, and Hongyan Wang for providing facilities and reagents; Aileen Sewell for manuscript editing and discussions, Beibei Ying and other faculty members at the Institute of Development Biology and Molecular Medicine of Fudan University for valuable discussions.

CONFLICT OF INTEREST

The authors have declared that no conflict of interest exists.

APPENDIX A. SUPPLEMENTARY DATA

Supplementary data related to this article can be found at http://dx.doi.org/10.1016/j.molmet.2017.03.003.

REFERENCES

[1] Kopelman, P.G., 2000. Obesity as a medical problem. Nature 404:635–643.
[2] Lawrence, M.C., Jivan, A., Shao, C., Duan, L., Goad, D., Zaganjor, E., et al., 2008. The roles of MAPKs in disease. Cell Research 18:436–442.
[3] Houseknecht, K.L., Zhu, A.X., Gnudi, L., Hamann, A., Zierath, J.R., Tozzo, E., et al., 1996. Overexpression of Ha-ras selectively in adipose tissue of transgenic mice. Evidence for enhanced sensitivity to insulin. Journal of Biological Chemistry 271:11347–11355.
[4] Pearce, L.R., Atanassova, N., Banton, M.C., Bottomley, B., van der Klaauw, A.A., Revelli, J.P., et al., 2013. KSR2 mutations are associated with obesity, insulin resistance, and impaired cellular fuel oxidation. Cell 155:765–777.
[5] Fernandez, M.R., Henry, M.D., Lewis, R.E., 2012. Kinase suppressor of Ras 2 (KSR2) regulates tumor cell transformation via AMPK. Molecular and Cellular Biology 32:3718–3731.
[6] Costanzo-Garvey, D.L., Pfluger, P.T., Dougherty, M.K., Stock, J.L., Boehm, M., Chaika, O., et al., 2009. KSR2 is an essential regulator of AMP kinase, energy expenditure, and insulin sensitivity. Cell Metabolism 10:366–378.
[7] Dougherty, M.K., Ritt, D.A., Zhou, M., Specht, S.I., Monson, D.M., Veenstra, T.D., et al., 2009. KSR2 is a calcineurin substrate that promotes ERK cascade activation in response to calcium signals. Molecular Cell 34:652–662.
[8] Yamanashi, Y., Tamura, T., Kanamori, T., Yamane, H., Nariuchi, H., Yamamoto, T., et al., 2000. Role of the rasGAP-associated docking protein p62(dok) in negative regulation of B cell receptor-mediated signaling. Genes and Development 14:11–16.
[9] Di Cristofano, A., Niki, M., Zhao, M., Karnell, F.G., Clarkson, B., Pear, W.S., et al., 2001. p62(dok), a negative regulator of Ras and mitogen-activated protein kinase (MAPK) activity, opposes leukemogenesis by p210(bcr-abl). Journal of Experimental Medicine 194:275–284.
[10] Hosooka, T., Noguchi, T., Kotani, K., Nakamura, T., Sakaue, H., Inoue, H., et al., 2008. Dok1 mediates high-fat diet-induced adipocyte hypertrophy and obesity through modulation of PPAR-gamma phosphorylation. Nature Medicine 14:188–193.
[11] Noto, S., Maeda, T., Hattori, S., Inazawa, J., Imamura, M., Asaka, M., et al., 1998. A novel human RasGAP-like gene that maps within the prostate cancer susceptibility locus at chromosome 1q25. FEBS Letters 441:127–131.
[12] McLaughlin, S.K., Olsen, S.N., Dake, B., De Raedt, T., Lim, E., Bronson, R.T., et al., 2013. The RasGAP gene, RASAL2, is a tumor and metastasis suppressor. Cancer Cell 24:365–378.

[13] Huang, Y., Zhao, M., Xu, H., Wang, K., Fu, Z., Jiang, Y., et al., 2014. RASAL2 down-regulation in ovarian cancer promotes epithelial-mesenchymal transition and metastasis. Oncotarget 5:6734—6745.
[14] Thorleifsson, G., Walters, G.B., Gudbjartsson, D.F., Steinthorsdottir, V., Sulem, P., Helgadottir, A., et al., 2009. Genome-wide association yields new sequence variants at seven loci that associate with measures of obesity. Nature Genetics 41:18—24.
[15] Leon-Mimila, P., Villamil-Ramirez, H., Villalobos-Comparan, M., Villarreal-Molina, T., Romero-Hidalgo, S., Lopez-Contreras, B., et al., 2013. Contribution of common genetic variants to obesity and obesity-related traits in mexican children and adults. PLoS One 8:e70640.
[16] Cheung, C.Y., Tso, A.W., Cheung, B.M., Xu, A., Ong, K.L., Fong, C.H., et al., 2010. Obesity susceptibility genetic variants identified from recent genome-wide association studies: implications in a Chinese population. The Journal of Clinical Endocrinology and Metabolism 95:1395—1403.
[17] Sordella, R., Jiang, W., Chen, G.C., Curto, M., Settleman, J., 2003. Modulation of Rho GTPase signaling regulates a switch between adipogenesis and myogenesis. Cell 113:147—158.
[18] Kilroy, G., Burk, D.H., Floyd, Z.E., 2009. High efficiency lipid-based siRNA transfection of adipocytes in suspension. PLoS One 4:e6940.
[19] Spandidos, A., Wang, X., Wang, H., Seed, B., 2010. PrimerBank: a resource of human and mouse PCR primer pairs for gene expression detection and quantification. Nucleic Acids Research 38:D792—D799.
[20] Ding, S., Wu, X., Li, G., Han, M., Zhuang, Y., Xu, T., 2005. Efficient transposition of the piggyBac (PB) transposon in mammalian cells and mice. Cell 122:473—483.
[21] Cui, J., Ding, Y., Chen, S., Zhu, X., Wu, Y., Zhang, M., et al., 2016. Disruption of Gpr45 causes reduced hypothalamic POMC expression and obesity. Journal of Clinical Investigation 126:3192—3206.
[22] Cohen, J.C., Horton, J.D., Hobbs, H.H., 2011. Human fatty liver disease: old questions and new insights. Science 332:1519—1523.
[23] Baker, R.G., Hayden, M.S., Ghosh, S., 2011. NF-kappaB, inflammation, and metabolic disease. Cell Metabolism 13:11—22.
[24] Fujisaka, S., Usui, I., Bukhari, A., Ikutani, M., Oya, T., Kanatani, Y., et al., 2009. Regulatory mechanisms for adipose tissue M1 and M2 macrophages in diet-induced obese mice. Diabetes 58:2574—2582.
[25] Camp, H.S., Tafuri, S.R., 1997. Regulation of peroxisome proliferator-activated receptor gamma activity by mitogen-activated protein kinase. Journal of Biological Chemistry 272:10811—10816.
[26] Hu, E., Kim, J.B., Sarraf, P., Spiegelman, B.M., 1996. Inhibition of adipogenesis through MAP kinase-mediated phosphorylation of PPARgamma. Science 274:2100—2103.
[27] Prusty, D., Park, B.H., Davis, K.E., Farmer, S.R., 2002. Activation of MEK/ERK signaling promotes adipogenesis by enhancing peroxisome proliferator-activated receptor gamma (PPARgamma) and C/EBPalpha gene expression during the differentiation of 3T3-L1 preadipocytes. Journal of Biological Chemistry 277:46226—46232.
[28] Kortum, R.L., Costanzo, D.L., Haferbier, J., Schreiner, S.J., Razidlo, G.L., Wu, M.H., et al., 2005. The molecular scaffold kinase suppressor of Ras 1 (KSR1) regulates adipogenesis. Molecular and Cellular Biology 25:7592—7604.
[29] Sale, E.M., Atkinson, P.G., Sale, G.J., 1995. Requirement of MAP kinase for differentiation of fibroblasts to adipocytes, for insulin activation of p90 S6 kinase and for insulin or serum stimulation of DNA synthesis. EMBO Journal 14:674—684.
[30] Bost, F., Aouadi, M., Caron, L., Even, P., Belmonte, N., Prot, M., et al., 2005. The extracellular signal-regulated kinase isoform ERK1 is specifically required for in vitro and in vivo adipogenesis. Diabetes 54:402—411.
[31] Donzelli, E., Lucchini, C., Ballarini, E., Scuteri, A., Carini, F., Tredici, G., et al., 2011. ERK1 and ERK2 are involved in recruitment and maturation of human mesenchymal stem cells induced to adipogenic differentiation. Journal of Molecular Cell Biology 3:123—131.

